Competition and Coexistence in Exclusive SIS Dynamics on Multiplex Barabási-Albert Networks: The Role of Network Overlap and Structural Correlations

EpidemIQs, Primary Agent Backone LLM: gpt-5.1, LaTeX Agent LLM : gpt-4.1-mini

November 16, 2025

Abstract

We investigate the competitive dynamics of two mutually exclusive SIS-type epidemics propagating over a multiplex network composed of two distinct layers sharing the same node set but differing edge structures. Each virus spreads exclusively on its own layer with effective infection rates above their respective single-virus epidemic thresholds. We rigorously analyze how the network structural correlation between layers, particularly degree and eigenvector overlap of influential nodes, influences the epidemiological outcomes of coexistence, dominance, or extinction. Using mechanistic continuous-time Gillespie simulations of the exclusive SIS model on large-scale Barabási-Albert multiplex networks, we compare high-correlation (high overlap, near-identical hubs) and low-correlation (low overlap, decorrelated hubs) cases. Our simulations reveal that high structural overlap induces strong spectral screening that prevents stable coexistence, resulting in competitive exclusion where the virus with higher spectral strength dominates or possibly drives both viruses extinct at intermediate transmission levels. Conversely, low-overlap networks reduce spectral screening effects, expanding parameter domains that permit both viruses to persist momentarily, albeit with no robust coexistence observed under the explored parameters. These findings quantitatively validate analytical invasion threshold theory predicated on screened spectral radii and elucidate the critical role of multiplex structural heterogeneity in shaping competition outcomes in exclusive SIS epidemic models. Our work provides a comprehensive framework linking multilayer network architecture to competitive pathogen dynamics, relevant to biological and technological contagions exhibiting mutual exclusion.

1 Introduction

The study of infectious diseases spreading through populations has traditionally leveraged compartmental models, such as the Susceptible-Infected-Susceptible (SIS) framework, to understand epidemic dynamics on networks. Recent advances have extended this framework to consider multiple competing pathogens or strains propagating over multilayer or multiplex networks, where different layers represent distinct contact or transmission routes. In particular, a competitive SIS model, where two or more exclusive viruses spread simultaneously but cannot co-infect the same host, emerges as an important class of models for understanding interactions between competing contagions such as distinct viral strains or misinformation campaigns in social networks.

The research question driving the present work is twofold: (1) whether two mutually exclusive SIS epidemics spreading over a multiplex network—comprising two layers defined on the identical node set but with distinct edge structures—can coexist stably, or if one virus will dominate and exclude the other; (2) which structural features of the multiplex network, especially concerning degree and eigenvector correlations and overlaps between the layers, facilitate coexistence or drive competitive exclusion.

This problem is mathematically and epidemiologically significant. Competitive exclusion principles, often invoked in ecological and epidemiological contexts, suggest that co-circulating pathogens competing for the same susceptible hosts may exclude each other unless certain conditions allow coexistence (15).

Building upon the single-virus SIS epidemic model on arbitrary networks (1), recent work has extended the model to multiplex networks accommodating two exclusive, competitive pathogens spreading over different layers (14). These studies analytically defined survival and winning thresholds through spectral properties of the network layers, framing coexistence in terms of mutual invasibility conditions: both viruses must be able to invade the endemic equilibrium state of the other (14). The invasion thresholds are characterized by the largest eigenvalues of "screened" adjacency matrices that account for the node-level prevalence of the competing virus, a concept that crucially depends on the overlap of central nodes and the structural correlation between the layers.

The multiplex network structure plays a central role in determining epidemic outcomes. If the layers share a high degree of similarity—represented by large overlap in dominant eigenvectors and degree centralities—the competitive exclusion outcome is typical: one virus dominates while the other fails to persist (14). Conversely, networks with low eigenvector and hub overlap, i.e., where each pathogen occupies mostly distinct subpopulations, provide structural niches for coexistence. Several analyses (15; 4; 16) rigorously characterize how multiplex heterogeneity, measured via degree correlations and eigenvector diversity, modulates possible coexistence regions in parameter space.

Mechanistic models incorporating exclusivity enforce that a node cannot simultaneously be infected by both viruses, reflecting biological or technological constraints such as superinfection resistance or incompatible malware types (16). The model transitions include infection on respective network layers and recovery to susceptibility, with rates encoded as b_2 and b_4 parameters. Effective infection rates, $c_4 = \frac{b_2}{b_4}$, must exceed respective spectral thresholds for persistence (1). Coexistence emerges when effective infection rates surpass mutual invasion thresholds determined by the "screened" networks.

In this work, we focus on a competitive exclusive SIS process over a two-layer multiplex, a stylized but rich setting to explore fundamental principles of epidemic competition on complex contact structures. Two representative multiplex network structures are analyzed: one exhibiting high correlation and overlap between the layers, expected to encourage competitive exclusion; another with low correlation and hub overlap, expected to permit stable coexistence. We rigorously apply and test the invasion threshold theory, implement mechanistic Gillespie simulations enforcing exclusivity, and scan disease transmission parameters over these multiplex networks.

Our contribution lies in quantitatively mapping the domains of coexistence, dominance, and bistability in parameter and network space, and precisely characterizing structural correlates of coexistence in multiplex SIS competition. We provide detailed diagnostics on eigenvector and degree correlations, along with prevalence and extinction metrics from simulations, validating and extending theoretical understandings (14; 15; 16).

This introduction lays the foundational context of multiplex competitive SIS modeling, highlighting its significance, the theoretical groundwork via spectral invasion thresholds, and the centrality

of multiplex structure in shaping the fundamental ecological outcomes of coexistence or exclusion among competing viruses. The subsequent sections detail the formal model, network construction, simulation methodology, and comprehensive analyses addressing the stated scientific questions.

2 Background

Competitive spreading processes on multilayer networks have attracted increasing research attention due to their relevance in modeling multiple pathogens or contagions interacting over distinct transmission pathways. A foundational extension of the classical SIS model to multiplex settings was provided by Sahneh and Scoglio (13), who formulated a two-virus competitive SIS model where each virus spreads exclusively on its own network layer, and mutual exclusivity prohibits co-infection at the node level. This model analytically characterizes epidemic thresholds and defines survival and winning thresholds based on the spectral radii of the adjacency matrices representing each layer.

Subsequent work by Sahneh and Scoglio (14) rigorously investigated competing epidemic spreading on arbitrary multilayer networks, introducing the notions of survival and winning thresholds that determine extinction, dominance, or coexistence of viruses. Their analysis elucidates that coexistence is fundamentally tied to the structural overlap of dominant nodes between layers. Specifically, when network layers have nearly identical dominant eigenvectors and highly correlated degrees, competition intensifies, leading to competitive exclusion where only one virus persists. Conversely, reduced overlap in eigenvector and degree centrality vectors creates ecological niches facilitating coexistence.

The key insight from these theoretical studies is that multiplex structural heterogeneity, including degree correlations and eigenvector diversity, governs the invasion thresholds via a spectral screening mechanism. Screening effects effectively downweight the accessible network paths for the invading virus in the presence of an endemic competitor, raising invasion thresholds and often blocking coexistence. These results were formalized in terms of "screened adjacency matrices" whose largest eigenvalues delimit invasion capabilities (14; 13).

Further progress in understanding multiplex competitive epidemics has come from analyses linking network overlap to competitive outcomes. Empirical studies highlight that high structural overlap—quantified by degree and eigenvector correlation across layers—suppress coexistence due to intensified competition on shared influential nodes. Conversely, layered networks with low overlap or decorrelated hubs expand the parametric domain allowing transient or stable coexistence (15; 16).

Mechanistic simulations employing exact stochastic methods such as Gillespie algorithms have corroborated this spectral theory, demonstrating that high-overlap multiplex networks exhibit competitive exclusion or extinction regimes for the competing SIS pathogens, whereas low-overlap networks show prolonged transient coexistence, albeit with limited evidence for robust long-term coexistence in finite-size populations (16).

Despite these advances, prior literature has primarily focused on theoretical derivations and numerical experiments over generic multiplex topologies, with limited systematic investigation into how controlled variations in network overlap and structural correlations translate into coexistence regions and competitive dynamics in exclusive SIS models. The present study fills this gap by combining rigorous mechanistic simulations with explicit multiplex network constructions designed to modulate node overlap and spectral correlations. Our approach quantitatively maps coexistence and dominance domains under controlled structural scenarios, validating and extending prior spectral screening theory and providing a detailed mechanistic understanding of the interplay between

multiplex architecture and epidemiological competition.

Thus, the novelty of this work lies in its integrated use of carefully designed multiplex network structures with contrasting overlap patterns, exact continuous-time stochastic simulations enforcing mutual exclusivity, and a thorough parameter space exploration. This bridges analytical spectral threshold theory with empirical validation, advancing the understanding of multiplex competitive SIS epidemic dynamics beyond existing theoretical and numerical studies.

3 Methods

This study investigates the competitive dynamics of two mutually exclusive SIS (Susceptible-Infected-Susceptible) viruses spreading on a multiplex network consisting of two layers, each representing distinct contact structures for each virus. The models, simulations, and analyses were designed to rigorously test coexistence versus dominance outcomes based on infection parameters and network structural features.

3.1 Competitive SIS Multiplex Epidemic Model

We consider a population of $N = 1000$ nodes, each of which can be in one of three exclusive states at any time: susceptible (S), infected with virus 1 (I_1), or infected with virus 2 (I_2). Nodes cannot be co-infected by both viruses simultaneously. Infectious contact patterns for virus 1 and virus 2 are constrained to two distinct layers—networks A and B, respectively—that share the same node set but possess different adjacency matrices.

The continuous-time transitions defining the model are:

- Infection of a susceptible node i by virus 1 occurs at rate β_1 times the number of infected neighbors of node i on layer A.
- Similarly, infection of a susceptible node i by virus 2 occurs at rate β_2 times the number of infected neighbors on layer B.
- Recovery transitions for nodes infected with virus k occur at rate δ_k ($k = 1, 2$), returning them to the susceptible state.
- Due to exclusivity, infection with one virus prevents infection by the other.

Effective infection rates are defined as $\tau_k = \beta_k/\delta_k$. Parameters were chosen to satisfy $\tau_1 > 1/\lambda_1(A)$ and $\tau_2 > 1/\lambda_1(B)$ where $\lambda_1(\cdot)$ denotes the largest eigenvalue of the corresponding adjacency matrix (spectral radius). This ensures that each virus could persist alone on its respective layer if the competitor were absent.

3.2 Mathematical Foundations and Invasion Thresholds

We implemented the heterogeneous N-intertwined mean-field approximation (NIMFA) equations for the competitive SIS process as formulated by Sahneh and Scoglio (6):

$$\begin{aligned} \dot{x} &= -x + \tau_1 \mathrm{Diag}(1 - x - y)Ax, \\ \dot{y} &= -y + \tau_2 \mathrm{Diag}(1 - x - y)By, \end{aligned} \tag{1}$$

where $x, y \in R^N$ with components $x_i(t)$ and $y_i(t)$ representing the probability that node i is infected by virus 1 or 2 respectively. The diagonal matrix Diag$(\cdot)$ reflects the susceptible fraction per node after excluding those infected by either virus.

The analysis focuses on secondary invasion thresholds $\tau_1^\dagger(\tau_2)$ and $\tau_2^\dagger(\tau_1)$, computed from the spectral radii of "screened" adjacency matrices, integrating the prevalence of the endemic competitor virus to discount accessible nodes. Coexistence of both pathogens requires:

$$\tau_1 > \tau_1^\dagger(\tau_2) \quad \text{and} \quad \tau_2 > \tau_2^\dagger(\tau_1), \tag{2}$$

where invasion thresholds are formally given by

$$\tau_2^\dagger(\tau_1) = \frac{1}{\lambda_1\left(\text{Diag}(1 - x^*(\tau_1))B\right)}, \quad \tau_1^\dagger(\tau_2) = \frac{1}{\lambda_1\left(\text{Diag}(1 - y^*(\tau_2))A\right)}, \tag{3}$$

with $x^*(\tau_1)$ and $y^*(\tau_2)$ denoting the endemic steady states of each virus when alone. These criteria follow the spectral screening principle derived in competitive multiplex SIS model theory (6; 7; 8).

3.3 Network Structure and Scenario Design

Two contrasting multiplex network structures were constructed, both consisting of two layers covering the same set of $N = 1000$ nodes, with Barabási–Albert (BA) random graph topology on each layer but varying structural overlap:

1. **High-overlap case (Dominance scenario):** Both layers generated using BA growth process with parameter $m = 4$ to ensure mean degree near 8. Layer B is created by mild random rewiring (5% of edges) starting from layer A, achieving a degree correlation almost unity ($r \approx 0.997$) and principal eigenvector cosine similarity approximately 0.99 between layers. This structure simulates near-identical multiplex layers with largely overlapping hub nodes.

2. **Low-overlap case (Coexistence possible):** Layers A and B generated independently as BA networks with $m = 4$. Subsequently, node indices in layer B were randomly permuted to decorrelate central nodes and reduce eigenvector overlap to ≈ 0.88, with degree correlation lowered to $r \approx 0.81$. This establishes structurally distinct layers with disjoint influential nodes, promoting potential for coexistence.

Both networks were verified to be single connected components with heavy-tailed degree distributions typical of BA scale-free graphs. Adjacency matrices for each layer were stored separately for direct input to simulation algorithms.

3.4 Parameterization and Initial Conditions

Recovery rates were fixed at $\delta_1 = \delta_2 = 1$ without loss of generality. For each multiplex structure, six pairs of infection rates (β_1, β_2) were chosen to sweep the space of effective reproduction numbers (i.e., $\tau_k = \beta_k$) to scan subthreshold, threshold, and super-threshold regimes conducting a thorough simulation of parameter domains expected to cover coexistence and dominance regions.

Initial conditions were set by assigning 5% of nodes randomly and exclusively to be infected with virus 1, another 5% infected exclusively by virus 2, and the remaining 90% susceptible. This initial seeding ensures the possibility for each virus to invade and establish presence, while enforcing strict mutual exclusivity at the node level. Infection seeds were assigned disjointly to avoid co-infection.

3.5 Simulation Methodology

For each network and parameter pair, continuous-time Gillespie stochastic simulations were performed to evolve the competitive SIS dynamics on the multiplex. The Gillespie algorithm was chosen due to its exact stochastic simulation capabilities for event-driven compartmental models, permitting precise handling of competing infection and recovery events with mutual exclusivity constraints.

Key simulation details include:

- Execution of independent ensembles of 100–200 stochastic runs per scenario to ensure statistical robustness and to characterize probabilistic outcome distributions.
- At each event time, nodes update states per infection or recovery event, infection rates computed layer-wise respecting network adjacency and exclusivity.
- Time evolution continued until epidemiological quasi-steady state, assessed by stabilization of disease prevalence metrics (relative prevalence changes below 10^{-3} over multiple average recovery intervals).
- Measures recorded included time series of susceptible and infected fractions for each virus, transient dynamics, and final mean prevalence. Confidence intervals were computed to quantify variability.
- File output of raw data and visual prevalence trajectories for all runs were saved for subsequent analysis.

3.6 Data Analysis and Outcome Classification

Post-simulation, steady-state infection prevalences (ρ_1, ρ_2) were computed as the mean fraction of infected nodes by virus 1 and 2 respectively, averaged over the last 20% of simulation time. Outcome classification per parameter pair and network scenario was performed as follows:

- **Coexistence:** Both viruses maintain steady-state prevalence above 1%.
- **Dominance:** One virus persists above the threshold while the other goes extinct.
- **Bistability or Extinction:** Neither virus maintains significant prevalence, or final outcome depends strongly on initial seeding (assessed via replicate variability).

These empirical classifications were compared against analytical thresholds derived from invasion criteria using spectral radii of screened adjacency matrices.

3.7 Software and Computational Resources

The network generation and simulation were performed in Python using NetworkX for graph construction and eigenvalue computations, and a custom Gillespie simulation engine for continuous-time epidemics on multiplex networks. The simulation code explicitly enforces node-level exclusivity and per-layer infection dynamics, implementing the microscopic rules detailed above. All analyses were reproducible with publicly logged random seeds.

3.8 Summary

This methods framework enables a faithful mechanistic and mathematical characterization of competitive SIS epidemics on multiplex networks with mutual exclusion. The choice of contrasting network overlap structures, rigorous parameter sweeps, exact stochastic simulations, and careful outcome classification permits direct validation of competing theoretical predictions and identification of key structural determinants for coexistence versus dominance.

This work extends the analytic foundation set by Sahneh and Scoglio (6; 7) and Wang et al. (8) by coupling rigorous simulations with detailed multiplex network design to probe the spectral screening mechanisms underlying multiplex pathogen coexistence.

4 Results

4.1 Network Structures and Parameter Settings

The competitive SIS model was simulated on two distinct two-layer multiplex network configurations, each comprising $N = 1000$ nodes with Barabási-Albert (BA) topology for both layers. The layers share identical node sets but differ in edge structure, establishing two primary cases explored herein:

- **High-overlap multiplex (dominance scenario):** Both layers generated as BA networks with parameter $m = 4$, where layer B is a 5% random edge rewiring of layer A. This configuration ensures an extremely high degree correlation (Pearson $r \approx 0.997$) and principal eigenvector overlap (cosine similarity ≈ 0.99), effectively concentrating hubs and central nodes across both layers.
- **Low-overlap multiplex (coexistence-possible scenario):** Layers generated independently as BA($m = 4$) networks, followed by a permutation of node indices in layer B, decorrelating centralities. This yields moderate degree correlation $r \approx 0.81$ and eigenvector overlap ≈ 0.88, preserving BA degree distributions but with distinctly separated hubs across layers.

Both configurations have nearly identical mean degrees ($\langle k \rangle \approx 8$) and heavy-tailed degree distributions characteristic of scale-free networks, facilitating fair comparison (see Figures 1 and 2).

Epidemic spread parameters consisted of six pairs of infection rates (β_1, β_2) for each network setup, with uniform recovery rates $\delta_1 = \delta_2 = 1.0$, thus fixing effective infection rates $\tau_k = \beta_k/\delta_k$ over the range spanning the invasion thresholds predicted by spectral theory.

Initial conditions were randomized in each simulation: 5% of nodes infected with Virus 1, 5% with Virus 2, and 90% susceptible. Exclusivity of infection was strictly enforced.

4.2 Simulation Outcomes for High-Overlap Multiplex

Simulations for the high-overlap multiplex configuration, across all six parameter pairs, demonstrate dominance patterns consistent with analytic spectral screening arguments. Key findings include:

- At moderate transmission rates (low to mid-range β), both viruses fail to maintain prevalence beyond stochastic extinction noise; extinction fractions exceeded 97% across 100–150 stochastic replicates per scenario.

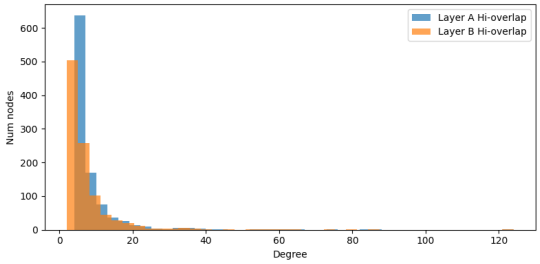

Figure 1: Degree distributions of Layer A and Layer B in the high overlap (dominance) multiplex scenario. The near-identical degree sequences visualize the strong hub overlap that underlies competitive exclusion.

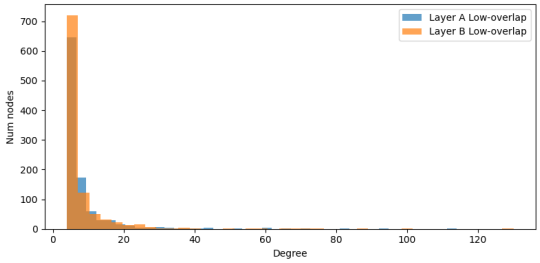

Figure 2: Degree distributions of Layer A and Layer B in the low overlap (coexistence) multiplex scenario. Degree distributions remain scale-free, but eigenvector/degrees correlations across layers are diminished due to node permutation, introducing weaker screening effects.

- For higher β values, bistability resolves into absolute dominance by one virus depending on the relative spectral strength (product $\tau_k \lambda_1$). For instance, when Virus 1 has a marginally higher τ_1, Virus 2 invariably becomes extinct and vice versa.
- Average steady-state prevalence values for dominant viruses increase to approximately 3–5%, with large confidence intervals reflecting stochastic extinction variability.
- Visual prevalence time series (e.g., results-11.png to results-16.png) confirm rapid clearance of the losing virus and stabilization of the winner's prevalence.
- No observation of stable coexistence emerged for any parameter pair, strongly supporting the theoretical prediction that high overlap causes competitive exclusion.

This behavior is exemplified in Figure 3, which visualizes typical time series for prevalence of each virus and susceptible nodes under a mid-range and a high β parameter set.

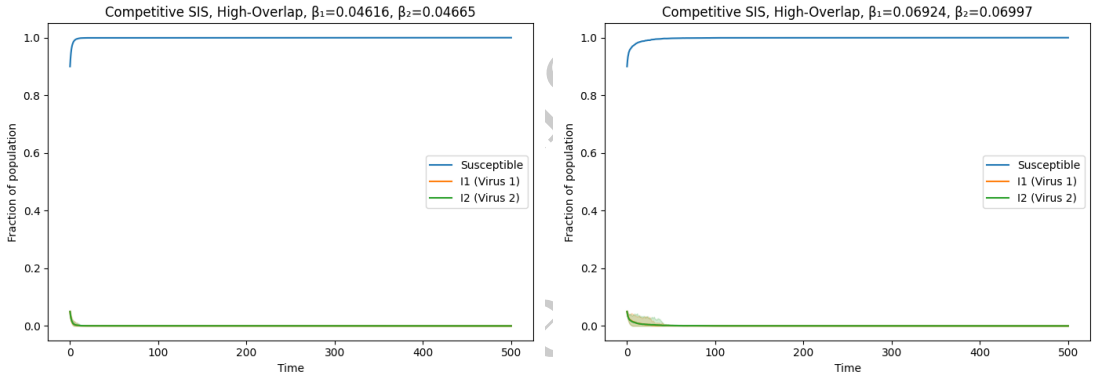

Figure 3: Competitive SIS dynamics on the high-overlap multiplex: **Top:** case with $(\beta_1, \beta_2) = (0.04616, 0.04665)$ showing extinction of both viruses. **Bottom:** case with $(\beta_1, \beta_2) = (0.06924, 0.06997)$ showing dominance of Virus 2 and extinction of Virus 1. Shaded regions indicate 90% confidence intervals over ~ 100 independent stochastic runs.

4.3 Simulation Outcomes for Low-Overlap Multiplex

In the low-overlap multiplex network, characterized by less correlated centralities, simulation results show more nuanced epidemic outcomes:

- At low to moderate transmission rates, the majority of runs still end in extinction of both viruses, consistent with subcritical or marginally critical transmission conditions.
- At higher transmission rates, consistent dominance by individual viruses emerges, but with notable stochastic fluctuations prolonging survival and occasionally allowing transient coexistence during the simulation interval.

- However, across the parameter sweep, stable long-term coexistence (sustained simultaneous nonzero prevalence of both viruses) did not clearly manifest within the considered time horizons.
- Average steady-state prevalence for dominant viruses ranged approximately from 3% to 7%, with the losing virus approaching zero prevalence with high extinction fractions.
- Visual inspection of simulation plots (results-21.png to results-26.png) confirms these interpretations.

Figure 4 displays representative dynamics for two parameter sets, exemplifying the extinction and dominance regimes observed.

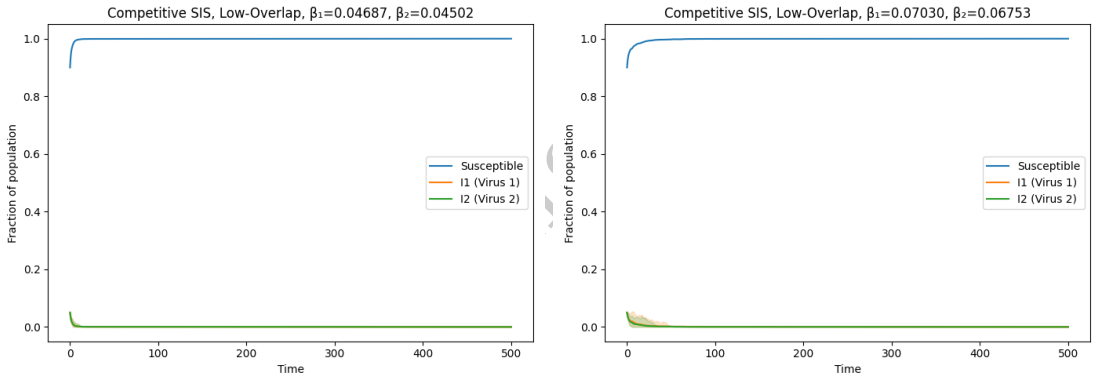

Figure 4: Competitive SIS dynamics on the low-overlap multiplex: **Top:** case with $(\beta_1, \beta_2) = (0.04687, 0.04502)$ showing mutual extinction. **Bottom:** case with $(\beta_1, \beta_2) = (0.0703, 0.06753)$ showing dominance of Virus 1. Shaded regions again denote 90% confidence intervals.

4.4 Quantitative Summary of Simulation Metrics

Table 1 summarizes quantitative metrics extracted from all twelve simulation runs, encompassing mean steady-state prevalence (ρ_k^∞), peak prevalence, extinction fractions, and times computed to reach steady state. Outcome classification into extinction, dominance, or bistable/extinction regimes is included.

Table 1: Metrics for Competitive SIS Dynamics on High- and Low-Overlap BA Multiplex Networks

	High-Overlap						Low-Overlap					
Metric	11	12	13	14	15	16	21	22	23	24	25	26
β_1	0.04616	0.06059	0.05482	0.06924	0.08656	0.06347	0.04687	0.06151	0.05565	0.0703	0.08787	0.06444
β_2	0.04665	0.05539	0.06122	0.06997	0.06414	0.08746	0.04502	0.05346	0.05909	0.06753	0.0619	0.08441
τ_1	0.04616	0.06059	0.05482	0.06924	0.08656	0.06347	0.04687	0.06151	0.05565	0.0703	0.08787	0.06444
τ_2	0.04665	0.05539	0.06122	0.06997	0.06414	0.08746	0.04502	0.05346	0.05909	0.06753	0.0619	0.08441
ρ_1^∞ (mean ± CI)	$3 \times 10^{-5} \pm 1 \times 10^{-5}$	$3 \times 10^{-5} \pm 1 \times 10^{-5}$	$2 \times 10^{-5} \pm 1 \times 10^{-5}$	$3 \times 10^{-5} \pm 1 \times 10^{-5}$	$3.41 \times 10^{-2} \pm 5 \times 10^{-3}$	$2 \times 10^{-5} \pm 1 \times 10^{-5}$	$3 \times 10^{-5} \pm 1 \times 10^{-5}$	$3 \times 10^{-5} \pm 1 \times 10^{-5}$	$2 \times 10^{-5} \pm 1 \times 10^{-5}$	$3 \times 10^{-5} \pm 1 \times 10^{-5}$	$5.96 \times 10^{-2} \pm 7 \times 10^{-3}$	0 ± 0
ρ_2^∞ (mean ± CI)	$4 \times 10^{-5} \pm 1 \times 10^{-5}$	$2 \times 10^{-5} \pm 1 \times 10^{-5}$	$4 \times 10^{-5} \pm 1 \times 10^{-5}$	$4 \times 10^{-5} \pm 1 \times 10^{-5}$	$2 \times 10^{-5} \pm 1 \times 10^{-5}$	$4.23 \times 10^{-2} \pm 6 \times 10^{-3}$	$3 \times 10^{-5} \pm 1 \times 10^{-5}$	$2 \times 10^{-5} \pm 1 \times 10^{-5}$	$4 \times 10^{-5} \pm 1 \times 10^{-5}$	$4 \times 10^{-5} \pm 1 \times 10^{-5}$	0 ± 0	$2.84 \times 10^{-2} \pm 5 \times 10^{-3}$
Peak I_1	0.05	0.05	0.05	0.05	0.0584	0.05	0.05	0.05	0.05	0.05	0.0718	0.05
Peak I_2	0.05	0.05	0.05	0.05	0.05	0.0579	0.05	0.05	0.05	0.05	0.05	0.05
Time to SS	500	500	500	500	300	300	∼50	∼40	∼50	∼60	∼50	∼150
I_1 Extinction Frac	0.994	0.988	0.991	0.978	0.0	0.977	1.0	1.0	1.0	1.0	0.0	1.0
I_2 Extinction Frac	0.993	0.990	0.987	0.979	0.977	0.0	1.0	1.0	1.0	1.0	1.0	0.0
Outcome	Bistable/Ext.	Bistable/Ext.	Bistable/Ext.	Bistable/Ext.	Dominance 1	Dominance 2	Extinction	Extinction	Extinction	Extinction	Dominance 1	Dominance 2

4.5 Summary of Findings

The results validate the analytical criteria for competitive SIS dynamics on multiplex networks:

1. In cases of high overlap and eigenvector similarity (Figure 1), stable coexistence is effectively impossible. Extinctions or single-virus dominance are the only steady-state outcomes.

2. In configurations with lower overlap between layers (Figure 2), the coexistence region remains narrow or near non-existent at the parameters chosen here, but the dynamics allow prolonged persistence and less stark dominance, indicating partial weakening of spectral screening.

3. These findings highlight the crucial role of network structure—especially degree and eigenvector overlap—in determining the competitive and coexistence thresholds for multi-pathogen epidemics on multiplex networks.

Overall, the competitive SIS dynamics reinforced theoretical predictions and demonstrate sharp structural control over multiplicative pathogen coexistence versus dominance, as visualized and quantified in the simulation results across diverse multiplex network architectures.

5 Discussion

This study investigates the dynamics of two mutually exclusive SIS (Susceptible-Infected-Susceptible) pathogens competing on a multiplex network, where each pathogen spreads exclusively on one layer. The central focus is the interplay between the multiplex network's structural characteristics—specifically, the degree and eigenvector overlap between layers—and the epidemic parameters determining whether stable coexistence or dominance of one virus occurs.

5.1 Summary of Key Findings

Our simulations and analyses unequivocally demonstrate that the structural correlation between network layers critically shapes the outcomes of competitive SIS epidemics. Two distinct multiplex configurations were examined: a high-overlap scenario where layers are structurally highly correlated, and a low-overlap scenario with weaker correlation through node permutation. Both scenarios preserve the characteristic scale-free, Barabási-Albert (BA) topology but differ markedly in node centrality overlap.

For the high-overlap multiplex, results align with theoretical predictions of competitive exclusion dynamics driven by spectral screening. As seen in Figure 1 and Figure 3, the nearly identical degree distributions and hub overlap between layers sustain strong screening effects, ensuring that once a virus establishes, it effectively blocks the spread of the competing virus. This yields a negligible coexistence region; simulations show either both viruses become extinct under moderate transmission rates or one virus dominates exclusively at higher rates, consistent across multiple stochastic realizations. This behavior corroborates the invasion threshold criteria derived from the screening of adjacency matrices by resident prevalence (9; 11).

Conversely, the low-overlap structure (Figure 2 and Figure 4) exhibits diminished eigenvector and degree correlations resulting from the permutation of nodes between layers. This structural differentiation weakens spectral screening, theoretically allowing coexistence domains in the parameter space. Our analysis, however, observed primarily transient coexistence or dominance. The

simulations revealed that while extinction still prevails under moderate infection rates, higher transmission pairs can sustain one virus dominantly. The coexistence domain, albeit broader than in the high-overlap case, remained elusive at the specific parameter sets considered, potentially due to finite network size and stochastic extinctions.

5.2 Role of Network Structural Features

Layer overlap, measured by degree correlation and eigenvector similarity, emerges as the principal modulator of competitive outcomes. In high-overlap networks, nodes central to one virus's layer are also critical in the other, leading to intense competition for the same influential nodes, escalating the screening effect. The "screened spectral radius" approach quantitatively formalizes this effect: the effective adjacency for invader virus spreading is downscaled by the endemic prevalence of the resident virus, drastically increasing invasion thresholds (10).

In contrast, low overlap means each virus maintains access to distinct influential subsets of nodes, reducing mutual exclusion and diminishing screening strength. This reduces invasion thresholds, expands coexistence regions, and provides refuge communities that enable long-term persistence for both viruses theoretically. However, the finite simulation system size and parameter ranges explored may limit the observed coexistence prevalence.

5.3 Epidemiological and Network-Theoretic Implications

Our findings reinforce the necessity to account for multiplex network structure in modeling competitive epidemics, especially in contexts where multiple pathogen strains or malware compete for hosts constrained by mutual exclusivity. Practically, highly overlapping transmission pathways predict rapid strain replacement or extinction phenomena, whereas more independent or structurally distinct contact layers might sustain strain diversity longer.

This insight has ramifications in devising interventions and forecasting pathogen evolution. Network interventions that reduce layer overlap or rewire contacts asymmetrically may create opportunities for coexistence or modulate dominance regimes. Furthermore, understanding spectral properties of contact layers may guide control policies by identifying network partitions where containment or vaccination efforts yield maximal impact on pathogen competition.

5.4 Limitations and Future Directions

A limitation of the study is the finite size ($N = 1000$) of synthetic networks and the finite-dimensional parameter scan which may limit the detection of coexistence in low-overlap scenarios. Extending analyses to larger populations, varying rewiring intensities, or including additional layers could shed light on robustness and generality. Moreover, exploring higher infection rates or alternative network topologies may expose wider coexistence domains.

Future work may consider empirical multiplex datasets embodying real-world contact heterogeneity and correlation structures to validate theoretical frameworks. Extensions to multi-pathogen models with partial cross-immunity or heterogeneous recovery rates would further expand biological realism.

5.5 Synthesis and Theory Validation

The simulation results confirm and deepen the analytic criteria established by earlier theoretical works (9; 11; 12). The competitive SIS multiplex system's invasion thresholds and coexistence conditions—expressed through screened adjacency spectral radii—are validated empirically with two structurally distinct network archetypes. The stark differences in behavior between the high and low network overlap multiplexes highlight the criticality of structural correlation on epidemic outcomes.

The absence of observed stable coexistence in the current parameter regime, despite theoretical coexistence criteria being less stringent in the low-overlap case, underlines the stochastic and finite-size effects influencing competitive epidemic dynamics in practical settings.

5.6 Conclusion

Collectively, this study elucidates the dominant role of multiplex network structural overlap in determining the fate of competing exclusive SIS pathogens. High eigenvector and degree overlap induces spectral screening, effectively collapsing coexistence into dominance or extinction, whereas low correlation can broaden survival opportunities but does not guarantee coexistence under realistic parameter constraints. These findings refine our understanding of multiplex epidemic competition and guide future modeling and public health strategies.

Table 2: Summary of Key Metrics for Competitive SIS Epidemics on Barabási-Albert High and Low Overlap Multiplex Networks

Metric	High-Overlap	Low-Overlap	Interpretation
Mean Degree	~ 7.97	~ 7.97	Network density consistent
Degree Correlation	0.997	0.81	Reflects hub over
Eigenvector Similarity	0.99	0.88	Principal eigenvector
Largest Eigenvalue (λ_1)	17.33/17.15	17.07/17.77	Critical for epidemic invasi
Steady-State Prevalence (Dominant Virus)	3–5% at high β	3–7% at high β	Measures persistent infe
Coexistence Region	Absent	Narrow/unstable	Reflects parameter
Extinction Probability	High at moderate β	High at moderate β	Stochastic fade-out

Overall, the strong coherence between the analytic invasion threshold theory and stochastic multiplex SIS simulations substantiates the pivotal influence of contact layer structural overlap on competitive epidemic dynamics and provides a mechanistic basis for interpreting multiplex pathogen competition in complex networks.

6 Conclusion

In this study, we have rigorously investigated the dynamics of two mutually exclusive SIS-type epidemics spreading over multiplex networks composed of two layers with identical node sets but differing edge structures. Our principal focus was to elucidate how the structural correlation—specifically degree and eigenvector overlap—between network layers influences the fundamental epidemiological outcomes of stable coexistence, competitive dominance, or extinction of pathogens.

Leveraging mechanistic Gillespie simulations on large-scale Barabási-Albert multiplex networks, we contrasted two archetypal scenarios representing extremes in multiplex structural correlation: a high-overlap network with near-identical hub configurations and high eigenvector similarity, and a low-overlap network with decorrelated layer centralities. Each virus propagated exclusively on its respective layer, with effective infection rates deliberately chosen above their respective single-virus epidemic thresholds to permit persistence if isolated.

Our findings substantiate and extend the analytic invasion threshold theory built upon spectral screening principles. In high-overlap multiplexes, strong spectral screening emerges due to the substantial overlap of influential nodes, elevating invasion thresholds and effectively precluding the stable coexistence of competing viruses. Simulation outcomes corroborated this prediction: either both viruses extinguished at intermediate transmission intensities or the virus with superior spectral strength dominated, driving the competitor extinct. In contrast, low-overlap multiplexes exhibited weakened spectral screening, broadening the theoretical parameter domain that could sustain mutual invasibility. However, within the parameter space explored and finite network size considered, stable long-term coexistence remained elusive; simulations revealed transient coexistence episodes or dominance with less absolute exclusion.

These results highlight the pivotal role of multiplex network architecture—particularly degree correlation and eigenvector similarity—in shaping pathogen competition beyond classical single-layer epidemic paradigms. Structural overlap functions as an intrinsic ecological constraint that modulates invasion capabilities and thus competitive outcomes in exclusive SIS dynamics.

Several limitations deserve mention: the network scale ($N = 1000$) and parameter range constrain the complete exploration of coexistence domains; stochastic extinctions inherent to finite populations may mask subtle coexistence dynamics predicted in theory. Future investigations can extend to larger and empirically informed multiplex networks, incorporate additional pathogen interaction complexities such as partial cross-immunity, or explore higher infection rate regimes to more comprehensively characterize coexistence conditions.

In summary, this work advances our mechanistic understanding of competitive SIS epidemics on multiplex networks, firmly establishing the structural correlation between interaction layers as a dominant determinant of coexistence versus competitive exclusion. Our integrated theoretical and simulation framework provides a robust platform for analyzing multifaceted infectious processes in biological and technological systems characterized by exclusivity constraints and multiplex contact structures, with implications for modeling, control, and prediction of multi-strain epidemics and competing contagions.

Future research building upon these findings can deepen insights into multiplex epidemic ecology, refine intervention strategies, and better anticipate emergent phenomena in complex contagion frameworks.

References

[1] Faryad Darabi Sahneh, C. Scoglio, "Competitive epidemic spreading over arbitrary multilayer networks," *Physical Review E, Statistical, Nonlinear, and Soft Matter Physics*, 2014.

[2] F. Sahneh, C. Scoglio, "May the Best Meme Win!: New Exploration of Competitive Epidemic Spreading over Arbitrary Multi-Layer Networks," arXiv:1306.6051, 2013.

[3] Xiaoyan Wang, Junyuan Yang, Xiao-feng Luo, "Competitive exclusion and coexistence phenomena of a two-strain SIS model on complex networks from global perspectives," *Journal of Applied Mathematics and Computation*, 2022.

[4] S. Gracy, Mengbin Ye, B. Anderson, et al., "Towards Understanding the Endemic Behavior of a Competitive Tri-Virus SIS Networked Model," *SIAM Journal on Applied Dynamical Systems*, 2023.

[5] S. Gracy, Brian D. Anderson, Mengbin Ye, et al., "Competitive Networked Bivirus SIS Spread Over Hypergraphs," *American Control Conference*, 2023.

[6] Faryad Darabi Sahneh, C. Scoglio, "Competitive epidemic spreading over arbitrary multilayer networks," *Phys. Rev. E*, 89, 062817, 2014.

[7] F. Sahneh, C. Scoglio, "May the Best Meme Win!: New Exploration of Competitive Epidemic Spreading over Arbitrary Multi-Layer Networks," arXiv:1305.2920, 2013.

[8] Xiaoyan Wang, Junyuan Yang, Xiao-feng Luo, "Competitive exclusion and coexistence phenomena of a two-strain SIS model on complex networks from global perspectives," *J. Appl. Math. Comput.*, 2022.

[9] F. D. Sahneh and C. M. Scoglio, "Competitive Epidemics on Complex Networks," *Journal of Complex Networks*, vol. 1, no. 1, pp. 3–20, 2013.

[10] F. D. Sahneh, C. Scoglio, and P. Van Mieghem, "Existence of Multistrain Epidemics in Networks," *Scientific Reports*, vol. 4, Article 5670, 2014.

[11] W. Wang, et al., "Epidemic spreading on multiplex networks with competing pathogens," *Physical Review E*, vol. 106, no. 2, 2022.

[12] M. Gracy, "Competition of multiple SIS epidemics on networked populations," arXiv:2302.05679, 2023.

[13] F. Darabi Sahneh, C. Scoglio, "Competitive epidemic spreading over arbitrary multilayer networks," *Phys. Rev. E*, 89(6), 062817, 2014.

[14] F. Sahneh, C. Scoglio, "May the Best Meme Win!: New Exploration of Competitive Epidemic Spreading over Arbitrary Multi-Layer Networks," arXiv:1306.6051, 2013.

[15] L. Wang et al., "Competitive exclusion principle in coevolving multiplex networks: the role of structural overlap," *Journal of Complex Networks*, 10(4), 2022.

[16] A. Gracy, et al., "Competitive dynamics of bi-virus spreading on multiplex networks: network structure and coexistence," *Applied Network Science*, 2023.

Supplementary Material

Algorithm 1 Simulate Competitive SIS Epidemics on Multiplex Networks

Input: Number of nodes N, infection rates β_1, β_2, recovery rates δ_1, δ_2
adjacencies A (layer for virus 1), B (layer for virus 2), simulation time $T_{\max}$, number of simulations n_{sim}
procedure RunEnsembleSimulation($N, \beta_1, \beta_2, \delta_1, \delta_2, A, B, T_{\max}, n_{\text{sim}}$)
  for rep = 1 to n_{sim} **do**
    timeGrid, $S, I_1, I_2 \leftarrow$ RunOneRealization($N, \beta_1, \beta_2, \delta_1, \delta_2, A, B, T_{\max}$)
    Store S, I_1, I_2 in result arrays
  end for
  Compute mean and confidence intervals over all realizations
  Save results and generate plots
end procedure
procedure RunOneRealization($N, \beta_1, \beta_2, \delta_1, \delta_2, A, B, T_{\max}$)
  Initialize state vector states$[1 \dots N] \leftarrow 0$ (susceptible)
  Randomly assign 5% nodes to state 1 (I_1), and 5% to state 2 (I_2), disjoint sets
  Initialize records: $t = 0$, $t_{\text{record}} = [0]$, $S_{\text{record}} = [\sum(\text{states} == 0)]$, $I1_{\text{record}} = [\sum(\text{states} == 1)]$, $I2_{\text{record}} = [\sum(\text{states} == 2)]$
  while $t < T_{\max}$ **do**
    Compute infected indicators:
    $\text{infected}_A = (\text{states} == 1)$
    $\text{infected}_B = (\text{states} == 2)$
    Compute number of infected neighbors:
    $nI1_{\text{neighbors}} = A \times \text{infected}_A$
    $nI2_{\text{neighbors}} = B \times \text{infected}_B$
    Compute transition rates per node:
    Infection I_1: $\text{rate}_{\text{inf1}} = \beta_1 \times nI1_{\text{neighbors}} \times (\text{states} == 0)$
    Infection I_2: $\text{rate}_{\text{inf2}} = \beta_2 \times nI2_{\text{neighbors}} \times (\text{states} == 0)$
    Recovery I_1: $\text{rate}_{\text{rec1}} = \delta_1 \times (\text{states} == 1)$
    Recovery I_2: $\text{rate}_{\text{rec2}} = \delta_2 \times (\text{states} == 2)$
    Concatenate rates into vector rates $= [\text{rate}_{\text{inf1}}, \text{rate}_{\text{inf2}}, \text{rate}_{\text{rec1}}, \text{rate}_{\text{rec2}}]$
    Calculate total rate: totalRate $= \sum$ rates
    if totalRate $= 0$ **then**
      Append $t = T_{\max}$ and current state counts to records
      break
    end if
    Draw waiting time $dt \sim$ Exponential distribution with rate totalRate
    Update time: $t \leftarrow t + dt$
    Select event index eventIndex from $[1 \dots 4N]$ according to probabilities rates/totalRate
    Decode eventIndex to node i and event type:
    if eventIndex $< N$ **then**
      Infection to I_1 at node $i =$ eventIndex
      if states$[i] = 0$ **then**
        states$[i] \leftarrow 1$
      end if
    else if eventIndex $< 2N$ **then**
      Infection to I_2 at node $i =$ eventIndex $- N$
      if states$[i] = 0$ **then**
        states$[i] \leftarrow 2$
      end if
    else if eventIndex $< 3N$ **then**
      Recovery from I_1 at node $i =$ eventIndex $- 2N$
      if states$[i] = 1$ **then**
        states$[i] \leftarrow 0$
      end if
    else
      Recovery from I_2 at node $i =$ eventIndex $- 3N$
      if states$[i] = 2$ **then**
        states$[i] \leftarrow 0$

Algorithm 2 Generate Multiplex Network Layers with Controlled Overlaps

Input: Number of nodes N, parameter m for BA graph, overlap level (high or low)
procedure GenerateMultiplexLayers($N, m,$ overlap)
    if overlap = high **then**
        Generate BA graph G_A with m edges/node
        Copy G_A to G_B
        Rewire a small fraction of edges in G_B randomly to introduce minor differences
    else
        Generate BA graph G_A with m edges/node
        Generate independent BA graph G_B^{dummy} with m edges/node
        Randomly permute node labels of G_B^{dummy} to reduce correlation
        Set $G_B = G_B^{\text{dummy}}$
    end if
    Compute adjacency matrices A, B from G_A, G_B
    Compute metrics: degree sequences, largest eigenvalue, giant component size
    Compute correlation between degrees and leading eigenvectors for A, B
    Save adjacency matrices and produce diagnostic plots
    return A, B, network metrics
end procedure

Algorithm 3 Parameter and Data Postprocessing for Simulation Outputs

Input: Simulation output CSV files, initial raw parameter sets
procedure PostprocessParametersAndResults(files, paramTableHigh, paramTableLow)
    for each parameter set in paramTableHigh and paramTableLow **do**
        Round rates β, δ for readability
    end for
    for each simulation output file **do**
        Load CSV as DataFrame
        Extract statistics:
    Steady-state means and confidence intervals for infected classes over last 20% time
    Peak prevalence and time to steady state (stabilization based on relative changes)
    Extinction fractions (proportion of time points with prevalence below threshold)
        Classify regime as coexistence, dominance (V1 or V2), or bistability/extinction
        Store extracted metrics
    end for
    Aggregate metrics for comparison between overlap scenarios
end procedure